END
DATE
FILMED

4 -- 79
DDC

1.0

4 5
5 0
5 6

2.8

2.5

1.1

3.2

3.6

4 0

2.2

2.0

1.8

1.25 1.4 1.6

MICROCOPY RESOLUTION TEST CHART
NATIONAL BUREAU OF STANDARDS-1963-A

LEVEL

Physical and Chemical Properties of Squarate Complexes. 2.

Mössbauer Spectroscopy and Magnetic Susceptibility Studies of Several Dimeric

and Trimeric Iron(III) Complexes Containing the Squarate Dianion

by

James T. Wrobleski and David B. Brown

Prepared for Publication

in

Inorganica Chimica Acta

DDC
RECEIVED
FEB 16 1979
C

University of Vermont

Department of Chemistry

Burlington, Vermont 05405

January 17, 1979

79 02 15 022

REPORT DOCUMENTATION PAGE		READ INSTRUCTIONS BEFORE COMPLETING FORM
1. REPORT NUMBER 12 (AD A048223)	2. GOVT ACCESSION NO.	3. RECIPIENT'S CATALOG NUMBER
4. TITLE *(and Subtitle)* "Physical and Chemical Properties of Squarate Complexes. 2. Mössbauer Spectroscopy and Magnetic Susceptibility Studies of Several Dimeric and Trimeric Iron(III) Complexes Containing the Squarate Dianion"		5. TYPE OF REPORT & PERIOD COVERED Technical Report
		6. PERFORMING ORG. REPORT NUMBER
7. AUTHOR(s) J. T. Wrobleski and D. B. Brown		8. CONTRACT OR GRANT NUMBER(s) N00014-75-C-0756
9. PERFORMING ORGANIZATION NAME AND ADDRESS Department of Chemistry University of Vermont Burlington, Vermont 05401		10. PROGRAM ELEMENT, PROJECT, TASK AREA & WORK UNIT NUMBERS
11. CONTROLLING OFFICE NAME AND ADDRESS Office of Naval Research Department of the Navy Arlington, Virginia 22217		12. REPORT DATE January 17, 1979
		13. NUMBER OF PAGES 26
14. MONITORING AGENCY NAME & ADDRESS*(if different from Controlling Office)*		15. SECURITY CLASS. *(of this report)* Unclassified
		15a. DECLASSIFICATION/DOWNGRADING SCHEDULE

16. DISTRIBUTION STATEMENT *(of this Report)*

This document has been approved for public release and sale; its distribution is unlimited

17. DISTRIBUTION STATEMENT *(of the abstract entered in Block 20, if different from Report)*

18. SUPPLEMENTARY NOTES

19. KEY WORDS *(Continue on reverse side if necessary and identify by block number)*

Squarate complexes, Iron polymers, Mössbauer spectroscopy, Magnetism

IRON 57

20. ABSTRACT *(Continue on reverse side if necessary and identify by block number)*

Products obtained by the reaction of certain bases with μ-dihydroxo-bis[squaratodiaquoiron(III)] dihydrate, $[Fe(C_4O_4)(H_2O)_2(OH)]_2 \cdot 2H_2O$, $\underline{I}$, have been isolated and studied by the complementary methods of ^{57}Fe Mössbauer spectroscopy and magnetic susceptibility. Reaction of $\underline{I}$ with pyridine or substituted pyridine bases gives materials with formula $[Fe(C_4O_4)(L)_2(OH)]_2 \cdot 2H_2O$ where L = pyridine, 4-methylpyridine, or 3-methylpyridine. The

79 02 15 022

$Fe_2(OH)_2$ bridging unit is maintained in these complexes as evidenced by their variable-temperature magnetic susceptibility behavior. The data are very well described with a HDVV $S_1 = S_2 = 5/2$ dimer model where $J = -8$ cm^{-1} and $g = 2.00$. Dimethylsulfoxide (DMSO) reacts with $\underline{I}$ to give a μ_3-oxo complex containing coordinated DMSO, $[Fe_3O(C_4O_4)_3(DMSO)_3(H_2O)_3](OH)$. Magnetic susceptibility data for this complex are analyzed with a HDVV $S_1 = S_2 = S_3 = 5/2$ trimer model by assuming equivalent spin sites. Results of this analysis give $J = -39$ cm^{-1} and $g = 2.00$. The proposed trimeric structure of this complex is also inferred from the presence of a strong infrared absorption near 550 cm^{-1} assigned to the Fe-O stretching mode, $\nu_{asym}(Fe_3O)$. Reaction of $\underline{I}$ with KOH in ethanol yields a material whose magnetic susceptibility versus temperature behavior is indicative of a $\underline{S}_1 = \underline{S}_2 = 5/2$ dimer with $J = -96$ cm^{-1} and $g = 2.00$. Presence of a strong infrared absorption at 820 and 750 cm^{-1}, assigned to the Fe-O-Fe stretching mode, $\nu_{asym}(Fe_2O)$ is additional evidence for the proposed μ-oxo structure for this complex, $[Fe(C_4O_4)(H_2O)_2]_2O$. Mössbauer spectral parameters for these ferric squarate complexes are consistent with proposed structures.

Physical and Chemical Properties of Squarate Complexes. 2.

Mössbauer Spectroscopy and Magnetic Susceptibility Studies of Several Dimeric and Trimeric

Iron(III) Complexes Containing the Squarate Dianion

James T. Wrobleski and David B. Brown[*]

Department of Chemistry, University of Vermont, Burlington, VT 05405, U.S.A.

Products obtained by the reaction of certain bases with μ-dihydroxo-bis[squaratodia-quoiron(III)] dihydrate, $[Fe(C_4O_4)(H_2O)_2(OH)]_2 \cdot 2H_2O$, $\underline{I}$, have been isolated and studied by the complementary methods of ^{57}Fe Mössbauer spectroscopy and magnetic susceptibility. Reaction of $\underline{I}$ with pyridine or substituted pyridine bases gives materials with formula $[Fe(C_4O_4)(L)_2(OH)]_2 \cdot 2H_2O$ where L = pyridine, 4-methylpyridine, or 3-methylpyridine. The $Fe_2(OH)_2$ bridging unit is maintained in these complexes as evidenced by their variable-temperature magnetic susceptibility behavior. The data are very well described with a HDVV $\underline{S}_1 = \underline{S}_2 = 5/2$ dimer model where $\underline{J} \approx -8$ cm^{-1} and g = 2.00. Dimethylsulfoxide (DMSO) reacts with $\underline{I}$ to give a μ_3-oxo complex containing coordinated DMSO, $[Fe_3O(C_4O_4)_3(DMSO)_3(H_2O)_3](OH)$. Magnetic susceptibility data for this complex are analyzed with a HDVV $\underline{S}_1 = \underline{S}_2 = \underline{S}_3 = 5/2$ trimer model by assuming equivalent spin sites. Results of this analysis give $\underline{J} = -39$ cm^{-1} and g = 2.00. The proposed timeric structure of this complex is also inferred from the presence of a strong infrared absorption near 550 cm^{-1} assigned to the Fe-O stretching mode, $\nu_{asym}(Fe_3O)$. Reaction of $\underline{I}$ with KOH in ethanol yields a material whose magnetic suscepti-bility versus temperature behavior is indicative of a $\underline{S}_1 = \underline{S}_2 = 5/2$ dimer with $\underline{J} = -96$ cm^{-1} and g = 2.00. Presence of a strong infrared absorption at 820 and 750 cm^{-1}, assigned to the Fe-O-Fe stretching mode, $\nu_{asym}(Fe_2O)$ is additional evidence for the proposed μ-oxo structure for this complex, $[Fe(C_4O_4)(H_2O)_2]_2O$. Mössbauer spectral parameters for these ferric squarate complexes are consistent with proposed structures.

Introduction

As part of our overall research effort towards understanding the structure and bonding in iron complexes of oxalate (1), squarate (2), and dihydroxybenzoquinone (3) dianions, we
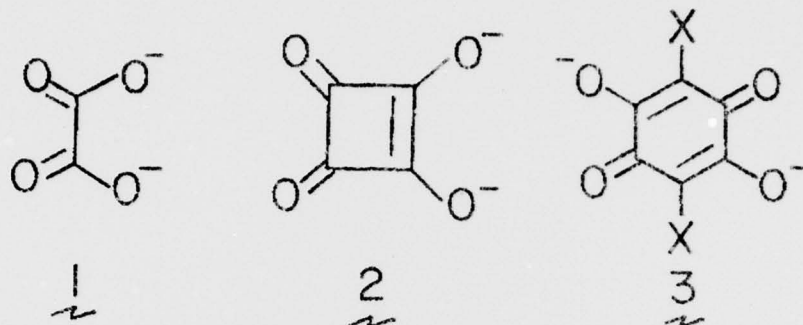
have recently reported [1] magnetic and spectroscopic data for the diaquo adduct of a dihydroxy-bridged iron(III) squarate (4). In the process of attempting to obtain single crystals of 4 suitable for diffraction studies we prepared several unique ferric squarate
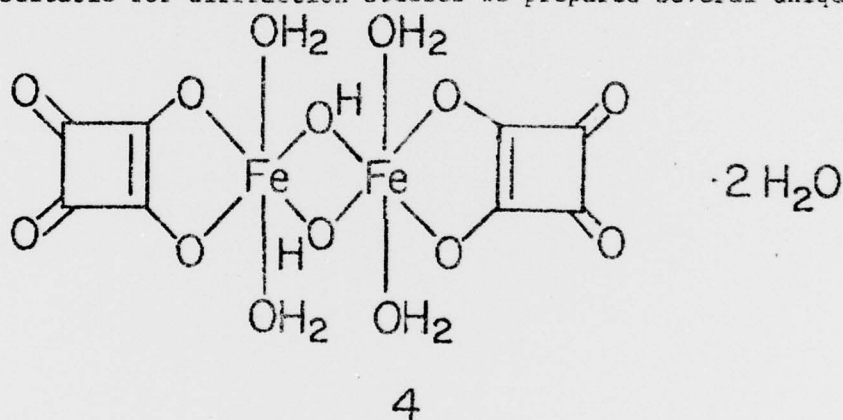
complexes which we have subsequently studied by a variety of techniques. These materials include pyridine and substituted-pyridine adducts analogous to 4, an oxo-bridged dimer with formula $[Fe(C_4O_4)(H_2O)_2]_2O$, and a μ_3-oxo triangular cluster with formula $[Fe_3O(C_4O_4)_3(DMSO)_3(H_2O)_3](OH)$ [2].

To date three types of complex containing 2 have been isolated and studied. In the first type, typified by 4 and the isostructural Al^{3+} [3], Cr^{3+} [3], V^{3+} [4], and Ti^{3+} [5] compounds, the squarate dianion acts as a singly-bidentate ligand. A second type of complex is illustrated by $[Cu_2(Et_5dien)_2(C_4O_4)](BPh_4)_2$ where Et_5dien is 1,1,4,7,7-pentaethyl-diethylenetriamine [6]. A schematic drawing of the assumed structure for this complex is shown in 5. In this material the squarate dianion is doubly bidentate. Apparently the
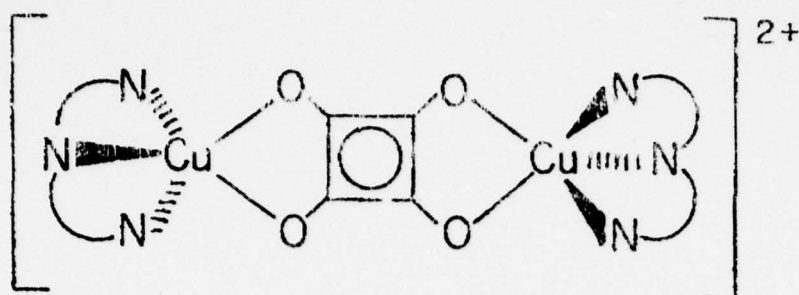
$$\underset{\displaystyle \sim}{5}$$

squarate ligand takes on this bis-chelate character in $[Fe_2(phenanthroline)_4(C_4O_4)]Cl_4$ [7] and the recently-discovered "white form" of $Fe(C_4O_4)(H_2O)_2$ [7]. The third type of squarate complex, of which $Ni(C_4O_4)(H_2O)_2$ [8] and the "yellow form" of $Fe(C_4O_4)(H_2O)_2$ [9] are iso-structural examples, consists of a three-dimensional network made up of divalent metal ions bridged by quadruply-monodentate squarate dianions.

Because of the variety of coordination modes possible for the squarate dianion, it seems appropriate to attempt to determine the factors which contribute to the stability of each of these boding types. We are particularly interested in the effect of these factors on the magnitude and mechanism of superexchange pathways in the squarate ligand and on the possible effects of coordinated squarate dianion on the magnetic and spectroscopic proper-ties of oligomers bridged by groups other than 2.

Experimental

Syntheses

The complexes $[Fe(C_4O_4)(OH)(L)_2]_2 \cdot 2H_2O$, where L = pyridine (py), 4-methylpyridine (4-Mepy), or 3-methylpyridine (3-Mepy), were prepared by stirring 1.00 g of $[Fe(C_4O_4)(OH)(H_2O)_2]_2 \cdot 2H_2O$ [1] in a solution of L containing approximately 5% water by volume. These mixtures were kept at 40°C until all the starting complex dissolved. The solutions were cooled to 0°C whereupon dark brown precipitates formed after several hours. The isolated products were kept at 0°C in a desiccator containing $CaSO_4$ in an atmosphere saturated with L. The yield of materials with the above method was normally within 5% of the theoretical. Analytical results are given in Table I.

TABLE I. Analytical Data

Compound	Calculated %				Observed %			
	Fe	C	H	N	Fe	C	H	N
[Fe(C$_4$O$_4$)(py)$_2$(OH)]$_2$·2H$_2$O	15.47	46.57	3.63	7.26	15.51	46.51	3.78	7.14
[Fe(C$_4$O$_4$)(4-Mepy)$_2$(OH)]$_2$·2H$_2$O	14.35	49.38	4.40	7.20	14.61	49.21	4.56	7.32
[Fe(C$_4$O$_4$)(3-Mepy)$_2$(OH)]$_2$·2H$_2$O	14.35	49.38	4.40	7.20	14.29	49.35	4.81	7.16
[Fe$_3$O(C$_4$O$_4$)$_3$(DMSO)$_3$(H$_2$O)$_3$](OH)	20.30	26.20	3.05		20.38	26.10	2.70	
[Fe(C$_4$O$_4$)(H$_2$O)$_2$]$_2$O	26.35	22.67	1.90		26.75	22.60	2.09	

The complex $[Fe_3O(C_4O_4)_3(DMSO)_3(H_2O)_3](OH)$ was prepared by refluxing a DMSO slurry of $[Fe(C_4O_4)(OH)(H_2O)_2]_2 \cdot 2H_2O$ until all the solid was dissolved. Cooling this solution to 5°C resulted in the formation of an orange-brown solid. This material was washed with cold DMSO followed by cold diethyl ether. The product was dried at room temperature in vacuum.

The complex $[Fe(C_4O_4)(H_2O)_2]_2O$ was prepared by stirring 1.00 g of $[Fe(C_4O_4)(H_2O)_2(OH)]_2$ $\cdot 2H_2O$ in warm ethanol containing a stoichiometric amount of KOH dissolved in 0.2 mL of water. After approximately 48 hours the starting dihydroxy-bridged complex had dissolved and a dark red-brown power was deposited in its place. This powder was dried at room temperature over $CaSO_4$ and stored in a sealed vial.

Magnetic Susceptibility Methods

Magnetic susceptibility data were collected at three field strengths by employing a conventional Faraday balance which has previously been described [10,11]. Temperature control was achieved by use of an Air Products APD-E Temperature Controller coupled to an Air Products CS-202 Displex He closed-cycle refrigerator. The ultimate temperature of this system was approximately 15K. Temperatures are reported accurate to ±0.2K. $Hg[Co(NCS)_4]$ was employed as the susceptibility standard [12]. Diamagnetic corrections were taken from a table of Pascal's constants [13]. The measured susceptibility of $K_2C_4O_4$ was taken as -30.6×10^{-6} cgsu [3].

Mössbauer Spectroscopy Methods

[57]Fe Mössbauer spectra were recorded on a constant-acceleration spectrometer which has been previously described [10,11]. The velocity scale was calibrated by using a 25 μm α-iron foil containing 430 μg [57]Fe/cm^2. Velocity scale linearity was normally within 1.5% in the range −6 to +6 mm/s. Experimental spectral data were treated in the normal manner [10] by assuming pure Lorentzian line shapes superimposed on a parabolic baseline.

Infrared Spectral Methods

Infrared spectra were recorded on a Beckman IR 20A instrument by using powdered samples dispersed in KBr pressed pellets. Spectra were also taken with samples dispersed

in nujol mulls supported on KBr plates. Reported band positions are accurate to approximately 5 cm^{-1}.

Analytical Methods

Iron content in these materials was determined by titration with either EDTA or dichromate. C, H, and N microanalyses were performed by Integral Microanalytical Laboratories, Inc., Raleigh, N.C.

Results and Discussion

The substituted pyridine complexes, $[Fe(C_4O_4)(L)_2(OH)]_2 \cdot 2H_2O$, are unstable with respect to loss of L. This loss of ligand is supressed by storing the materials in a desiccator containing a small amount of L. In order to obtain magnetic susceptibility and Mössbauer data for these materials it was necessary to cool the samples to 5°C in the apparatus before evacuating the sample compartment. Following a rapid evacuation the sample dewar was filled with helium gas to 1.1 atm. These precautions were sufficient to prevent detectable (<1%) loss of coordinated L. The DMSO addition product, $[Fe_3O(C_4O_4)_3(DMSO)_3(H_2O)_3](OH)$, was stable to loss of DMSO if kept below 0°C. After several months at 0°C, however, significant amounts of a dark brown material formed with concomitant formation of free DMSO. Consequently, we found it necessary to prepare this material immediately prior to performing the measurements. Finally, we have observed no change in samples of $[Fe(C_4O_4)(H_2O)_2]_2O$ stored at room temperature for six months.

Magnetic Susceptibility Studies

Experimental magnetic susceptibilities and effective magnetic moments for $[Fe(C_4O_4)(py)_2(OH)]_2 \cdot 2H_2O$, $[Fe(C_4O_4)(4-Mepy)_2(OH)]_2 \cdot 2H_2O$, and $[Fe(C_4O_4)(3-Mepy)_2(OH)]_2 \cdot 2H_2O$ are presented in Tables II, III, and IV, respectively. These data for the py complex are plotted in Figure 1. The general character of the susceptibility versus T plot is typical of the behavior expected for an $\underline{S}_1 = \underline{S}_2 = 5/2$ antiferromagnetic spin-exchange dimer. These data have therefore been numerically fit to the appropriate partition function [1] for an $\underline{S}_1 = \underline{S}_2 = 5/2$ dimer within the Heisenberg-Dirac-Van Vleck formalism (isotropic spin

TABLE II.   Magnetic Susceptibility Data for $[Fe(C_4O_4)(py)_2(OH)]_2 \cdot 2H_2O$

T, K	χ_M'(obsd) x 10^5 [a]	χ_M'(calcd) x 10^5 [b]	$\bar{\mu}_{eff}/Fe, \mu_B$
298.6	2278	2281	5.22
281.8	2380	2378	5.18
270.6	2247	2447	4.93
259.2	2520	2521	5.11
238.1	2673	2667	5.04
221.2	2789	2795	4.97
215.0	2841	2845	4.94
209.6	2890	2889	4.92
200.0	2970	2969	4.87
190.0	3061	3057	4.82
180.0	3145	3147	4.76
170.0	3230	3241	4.69
160.0	3331	3337	4.62
150.0	3440	3435	4.54
140.0	3535	3534	4.45
130.0	3630	3632	4.34
120.0	3730	3728	4.23
110.0	3831	3818	4.11
100.0	3900	3900	3.95
90.0	3970	3968	3.78
80.0	4015	4017	3.58
75.0	4030	4033	3.48
70.0	4041	4043	3.36
65.0	4044	4044	3.24
60.0	4036	4038	3.11
55.0	4020	4023	2.97
50.0	4002	3999	2.83
46.0	3970	3973	2.70
42.0	3940	3939	2.57
38.0	3895	3896	2.43
36.0	3877	3871	2.36

32.0	3840	3810	2.22
28.0	3720	3730	2.04
23.0	3591	3590	1.82
22.0	3555	3554	1.77
21.0	3511	3514	1.72
20.0	3468	3470	1.67
19.0	3410	3420	1.61
18.0	3366	3365	1.56
17.0	3302	3302	1.50
16.0	3235	3230	1.44
15.7	3205	3206	1.42

[a] M.Wt. = 722.23, χ^{dia} = −303 x 10^{-6} cgsu. [b] Calcd for $\underline{J}$ = −8.0 cm^{-1} and g = 2.00.

TABLE III. Magnetic Susceptibility Data for $[Fe(C_4O_4)(4\text{-Mepy})_2(OH)]_2 \cdot 2H_2O$

T, K	$\chi_M'(obsd) \times 10^5$ [a]	$\chi_M'(calcd) \times 10^5$ [b]	$\bar{\mu}_{eff}/Fe, \mu_B$
299.5	2251	2230	5.19
278.6	2340	2345	5.11
253.0	2600	2500	5.13
223.1	2700	2703	4.91
205.9	2836	2831	4.83
188.5	2975	2968	4.74
168.4	3139	3134	4.60
150.0	3299	3291	4.45
131.2	3450	3450	4.25
120.0	3535	3539	4.12
100.0	3670	3673	3.83
90.0	3786	3722	3.69
80.0	3741	3753	3.46
75.0	3765	3761	3.36
70.0	3766	3762	3.25
65.0	3760	3757	3.13
60.0	3742	3745	3.00
55.0	3735	3726	2.87
50.0	3710	3699	2.72
45.0	3660	3663	2.57
40.0	3610	3615	2.40
36.0	3568	3567	2.27
33.0	3522	3522	2.16
30.0	3475	3468	2.04
26.0	3396	3376	1.88
22.0	3299	3247	1.70
18.4	3210	3079	1.54

[a] M.Wt. = 778.34, $\chi^{dia} = -351 \times 10^{-6}$ cgsu. [b] Calcd for $\underline{J} = -8.6$ cm^{-1} and g = 2.00.

TABLE IV. Magnetic Susceptibility Data for $[Fe(C_4O_4)(3-Mepy)_2(OH)]_2 \cdot 2H_2O$

T, K	$\chi'_M(obsd) \times 10^5$ [a]	$\chi'_M(calcd) \times 10^5$ [b]	$\bar{\mu}_{eff}/Fe, \mu_B$
289.9	2368	2347	5.24
268.1	2496	2482	5.17
254.2	2580	2575	5.12
231.8	2740	2738	5.04
211.7	2880	2900	4.94
200.0	2996	3001	4.89
180.1	3180	3184	4.79
160.0	3380	3382	4.65
150.0	3489	3484	4.57
130.0	3690	3692	4.38
110.0	3872	3891	4.13
100.0	4010	3978	4.00
90.0	4050	4055	3.82
80.0	4112	4112	3.63
70.0	4160	4144	3.41
60.0	4130	4145	3.15
50.0	4101	4109	2.86
40.0	4000	4030	2.53
35.0	3950	3969	2.35
30.0	3890	3885	2.16
28.0	3846	3842	2.08
26.0	3820	3793	1.99
24.0	3760	3735	1.90
22.0	3700	3666	1.80
20.0	3680	3583	1.72
19.2	3600	3544	1.66
18.0	3520	3478	1.59
16.8	3500	3402	1.53

[a] M.Wt. = 778.34, $\chi^{calc} = -351 \times 10^{-6}$ cgsu. [b] Calcd for $\underline{J} = -7.8$ and g = 2.00.

Hamiltonian, $\underline{H} = -\underline{J}\Sigma\underline{S}_i\underline{S}_j$) with g constrained at 2.00. This single parameter equation best describes the experimental data of Figure 1 if the exchange parameter, $\underline{J}$, is set at -8.0 cm^{-1}. Similarly, excellent agreement between experiment and theory is found for the 4-Mepy and 3-Mepy adducts if $\underline{J} = -8.6$ and -7.8 cm^{-1}, respectively. Although there is no significant deviation from the theoretical curves at low temperatures for the py complex, we do observe slight positive deviations at T < 30K for the 4-Mepy and 3-Mepy derivatives. Inclusion of a susceptibility contribution from a $\underline{S} = 5/2$ monomeric impurity obeying Curie Law magnetism results in an improved fit to the data. The necessary correction is 0.08 and 0.04% impurity for the 4-Mepy and 3-Mepy complexes, respectively [14].

Exchange parameters for these complexes are nearly the same as that reported for $[Fe(C_4O_4)(H_2O)_2(OH)]_2\cdot 2H_2O$ ($\underline{J} = -7.0$ cm^{-1} [9] and $\underline{J} = -6.9$ cm^{-1} [1]) indicating that the structural integrity of the $Fe_2(OH)_2$ unit has been maintained in converting the aquo to the pyridine adducts. Structural and magnetic susceptibility studies have delineated the approximate bounds of $\underline{J}$ for dihydroxo-bridged Fe(III) dimers to lie in the range -7 to -15 cm^{-1}. Representative values are: $[(CH_3)_2NC_7H_2NO_4(H_2O)Fe(OH)]_2\cdot 2H_2O$ ($\underline{J} = -11.7$ cm^{-1}) [15], $[Dipic(H_2O)Fe(OH)]_2$ ($\underline{J} = -11.4$ cm^{-1}) and $[Chel(H_2O)Fe(OH)]_2\cdot 4H_2O$ ($\underline{J} = -7.3$ cm^{-1}) [16], $[Fe(salgly)(OH)]_2$ ($\underline{J} = -15$ cm^{-1}) [17], and $[(Pic)_2Fe(OH)]_2$ ($\underline{J} = -8.0$ cm^{-1}) [18].

Experimental magnetic susceptibilities and effective magnetic moments for $[Fe_3O(C_4O_4)_3(DMSO)_3(H_2O)_3](OH)$ are given in Table V. These data are plotted in Figure 2 and show a steady decrease in $\bar{\mu}_{eff}$ with decreasing temperature in the interval 300 to 100K. From 100 to 30K $\bar{\mu}_{eff}$ decreases more rapidly, then starts to level off at 30K. Such behavior is reminescent of the magnetic susceptibility behavior of μ_3-oxo Fe(III) trimers in which the intratrimer exchange parameter is near -30 cm^{-1} [19]. The data of Figure 2 were fit to equation 1 which is appropriate for an exchange-coupled system of three equivalent $\underline{S} = 5/2$ ions.

$$\chi_M(\text{trimer}) = \frac{N\beta^2 g^2}{4\underline{kT}} \; \frac{340e^{63x} + 455e^{48x} + 429e^{35x} + 330e^{24x} + 210e^{15x} + 105e^{8x} + 20e^{3x} + 1}{4e^{63x} + 7e^{48x} + 9e^{35x} + 10e^{24x} + 10e^{15x} + 9e^{8x} + 4e^{3x} + 1} \quad (1)$$

where the symbols have their usual meanings and $x = \underline{J}/\underline{kT}$ [20]. Theoretical curves obtained

TABLE V. Magnetic Susceptibility Data for $[Fe_3O(C_4O_4)_3(DMSO)_3(H_2O)_3](OH)$

T, K	$\chi'_M(obsd) \times 10^5$ [a]	$\chi'_M(calcd) \times 10^5$ [b]	$\bar{\mu}_{eff}/Fe$, μ_B
292.4	1196	1241	3.05
292.1	1203	1242	3.06
281.1	1229	1258	3.04
271.6	1233	1273	2.99
260.8	1240	1290	2.94
250.5	1255	1307	2.89
240.1	1258	1325	2.84
228.7	1284	1346	2.80
217.3	1291	1367	2.74
205.9	1324	1390	2.70
194.7	1339	1413	2.64
182.7	1364	1439	2.58
171.5	1394	1465	2.52
159.8	1401	1493	2.44
147.6	1441	1525	2.38
135.5	1481	1559	2.31
124.2	1547	1594	2.26
112.0	1606	1636	2.19
99.8	1660	1685	2.10
86.9	1767	1748	2.02
77.5	1865	1806	1.96
66.8	1982	1893	1.88
57.4	2147	2002	1.81
51.9	2231	2090	1.76
46.1	2396	2218	1.72
39.6	2608	2433	1.66
36.7	2721	2566	1.63
33.8	2860	2733	1.60
30.0	3101	3020	1.58
28.0	3270	3212	1.56
26.0	3460	3439	1.55
24.0	3635	3710	1.52
22.0	3928	4036	1.52
20.0	4257	4433	1.51
19.0	4527	4664	1.51

[a] M.Wt. = 825.12, χ^{dia} = -222 x 10^{-6} cgsu. [b] Calcd for $\underline{J}$ = -39.0 and g = 2.00 with 4.0% monomeric high spin $\underline{S}$ = 5/2 component.

with this equation deviated significantly from the experimental data below 100K. We therefore chose to describe the data by incorporating a term to account for the possible presence of a $\underline{S}$ = 5/2 monomeric impurity with molecular weight equal to 1/3 the trimer molecular weight. Expression 2 is the appropriate equation where $\underline{Z}$ is defined as the fraction of the experimental susceptibility partitioned to the trimer and χ_M(monomer) is

$$\chi_M(\text{obsd}) = \underline{Z}\chi_M(\text{trimer}) + 3(1 - \underline{Z})\chi_M(\text{monomer}) \tag{2}$$

4.376/T. The smooth curves in Figure 2 represent best fits of equation 2 to the data where $\underline{J}$ = -39.0, g = 2.00, and $\underline{Z}$ = 0.96 (4% $\underline{S}$ = 5/2 Curie law contaminant).

The formulation of this material as a trimeric cluster is consistent with the analytical and spectroscopic data (vide infra), and the parameters from the magnetic data fits are both physically realistic and acceptably model the essential features of the susceptibility curves (Figure 2). However, other structural models are possible, and we have consequently attempted to fit the data to a dimer expression similar to 2 (molecular weight dimer = 2/3 molecular weight trimer). With $\underline{J}$ = -49.5 cm^{-1}, g = 2.00 (constrained), and $\underline{Z}$ = 0.87 (13% impurity) this dimer model yields a statistically better fit to the data than does the trimer model. We believe that this is fortuitous agreement, because the value of $\underline{J}$ is physically unrealistic.

Table VI contains experimental magnetic susceptibilities and effective magnetic moments for [Fe(C$_4$O$_4$)(H$_2$O)$_2$]$_2$O. These data are plotted in Figure 3. The very strong temperature dependence of $\bar{\mu}_{eff}$ is consistent with a large antiferromagnetic spin-exchange interaction in this complex. Such magnetic behavior is typical of that observed for oxo-bridged ferric complexes [21-24]. The magnetism of these oxo-bridged systems is understandable in terms of a HDVV $\underline{S}_1$ = $\underline{S}_2$ = 5/2 dimer with exchange parameters near -100 cm^{-1} [25]. The data for [Fe(C$_4$O$_4$)(H$_2$O)$_2$]$_2$O were fit to this model resulting in best fit values of $\underline{J}$ = -96 cm^{-1} and g = 2.00. These parameters were used to calculate the theoretical curve shown in Figure 3. The discrepancy between experimental and calculated values does not exceed 0.8% except for points below 25K. Here, as before, inclusion of a Curie $\underline{S}$ = 5/2 monomeric impurity improves the low-temperature fit. Only 0.01% of this paramagnetic

TABLE VI. Magnetic Susceptibility Data for $[Fe(C_4O_4)(H_2O)_2]_2O$

T, K	$\chi_M'(obsd) \times 10^6$ [a]	$\chi_M'(calcd) \times 10^6$ [b]	$\bar{\mu}_{eff}/Fe, \mu_B$
291.2	3036	3029	1.88
280.6	3001	3001	1.84
269.1	2980	2972	1.79
254.2	2915	2929	1.72
231.0	2860	2861	1.63
218.6	2805	2812	1.57
200.2	2730	2730	1.48
180.9	2630	2634	1.38
171.6	2582	2571	1.33
152.4	2410	2408	1.21
130.6	2142	2167	1.06
119.1	1998	1996	0.98
101.1	1650	1651	0.82
96.2	1545	1532	0.77
80.4	1096	1101	0.59
71.2	850	821	0.49
60.0	470	489	0.34
50.0	210	241	0.20
45.0	119	143	0.15
40.0	80	71	0.11
35.0	40	34	0.07
30.0	10	12	0.03
26.0	8	2	0.03
22.0	6	<1	0.02
18.0	6	<1	0.02
17.0	10	<1	0.03
16.0	15	<1	0.03
15.7	21	<1	0.04

[a] M.Wt. = 423.84, χ^{dia} = -112 x 10^{-6} cgsu.   [b] Calcd for $\underline{J}$ = -96.0 cm^{-1} and g = 2.00.

monomer is necessary to model the data over the entire temperature range studied. A recent compilation [25] of exchange parameter values for oxo-bridged Fe(III) dimers points out that for these complexes $\underline{J} = -100 \pm 15$ cm^{-1}. The strong link between this value and the existence of the oxo-bridge in ferric complexes lends support to our suggestion for the structure of this complex.

Mössbauer Spectral Studies

Iron-57 Mössbauer spectra were recorded at 300K and approximately 20K for each of these compounds. The parameters which result from curve-fitting analyses are given in Table VII. Approximately two million counts per channel were collected for each spectrum. Because the average percent transmission of these spectra was 10%, the spectral signal-to-noise ratio exceeded 17 in all cases. Chemical isomer shifts, δ, for these compounds range from +0.32 to +0.42 mm/s, relative to α-Fe, at 300K. This range lies within established bounds for high-spin ferric complexes; +0.25 to +0.60 mm/s [26]. The quadrupole splitting parameters, ΔE_Q, listed in Table VII are also consistent with the presence of high-spin ferric ion in these complexes. In addition, the normal line-width and area ratios of the quadrupole-split components add no complication to the interpretation of the spectra.

It is worth noting that the ΔE_Q parameters for the di-μ-hydroxo complexes listed in Table VII are significantly larger than ΔE_Q observed for $[Fe(C_4O_4)(H_2O)_2(OH)]_2 \cdot 2H_2O$; $\Delta E_Q \leqq 0.16$ mm/s [1]. This increase in ΔE_Q is most likely a reflection of the larger electric field gradient tensor in the FeO_4N_2 relative to the FeO_6 chromophore. These larger values of ΔE_Q therefore lend support to our proposed structure for these complexes.

The Mössbauer spectral parameters for $[Fe_3O(C_4O_4)_3(DMSO)_3(H_2O)_3](OH)$ are similar to those observed for μ_3-oxo trimers whose structures have been established (see [19] for example). Thus for $[Fe_3O(CH_3CO_2)_6(H_2O)_3]Cl \cdot 5H_2O$ at 300K δ = +0.42 and ΔE_Q = 0.55 mm/s. Although it is common to observe an _increase_ of the line widths at low temperatures for ferric μ_3-oxo trimers [19], presumably due to certain relaxation effects, we detect no linewidth changes greater than 0.04 mm/s in the experimental temperature range.

TABLE VII. Mössbauer Data

Compound	T, K	δ, mm/s [a]	ΔE_Q, mm/s	Γ_1/Γ_2 [b]	A_1/A_2 [c]
$[Fe(C_4O_4)(py)_2(OH)]_2 \cdot 2H_2O$	300	0.41	0.58	0.89	0.91
	18	0.43	0.62	1.01	0.96
$[Fe(C_4O_4)(4-Mepy)_2(OH)]_2 \cdot 2H_2O$	300	0.38	0.55	0.93	0.96
	17	0.44	0.60	1.00	0.98
$[Fe(C_4O_4)(3-Mepy)_2(OH)]_2 \cdot 2H_2O$	300	0.40	0.53	0.92	1.00
	20	0.41	0.55	0.97	1.01
$[Fe_3O(C_4O_4)_3(DMSO)_3(H_2O)_3](OH)$	300	0.38	0.86	0.96	0.98
	20	0.42	0.91	1.00	1.02
$[Fe(C_4O_4)(H_2O)_2]_2O$	300	0.32	0.67	0.85	0.93
	15	0.37	0.76	0.98	1.00

[a] Relative to α-Fe foil. [b] Ratio of low to high energy absorption line widths. [c] Ratio of areas of low to high energy absorptions.

The Mössbauer parameters for $[Fe(C_4O_4)(H_2O)_2]_2O$ are consistent with those previously reported for oxo-bridged ferric dimers [27]. Although we observe a small temperature-dependent line width ratio in the temperature range 300 to 15K (Table VII) there is no compelling reason to presume this arises from relaxation or similar effects. However certain μ-oxo ferric complexes do indeed display characteristic line width and line intensity asymmetry which has been interpreted in several ways [25].

Infrared Spectral Studies

The infrared spectra of these ferric squarate complexes provide compelling support for our structural proposals. Several representative spectra are shown in Figure 4. The essential features of the spectrum of $[Fe(C_4O_4)(H_2O)_2(OH)]_2 \cdot 2H_2O$ are also found in the spectra of the analogous $[Fe(C_4O_4)(L)_2(OH)]_2 \cdot 2H_2O$ complexes. Additional bands which may be assigned to coordinated pyridine and methylpyridine are, of course, present in these spectra.

The spectra of all the di-μ-hydroxo complexes possess a very diffuse, moderately strong band envelope centered at 3100 cm^{-1} and several broad, structured bands in the range 600 to 900 cm^{-1}. These absorptions are associated with stretching and deformation O-H modes of coordinated and lattice water. A deformation mode due to bridging hydroxide is anticipated near 900 cm^{-1} [28], and we have assigned this mode to a weak, broad absorption centered at 850 cm^{-1} in $[Fe(C_4O_4)(H_2O)_2(OH)]_2 \cdot 2H_2O$ [1]. We observe similar bands at 850 ± 15 cm^{-1} in the spectra of the pyridine and methylpyridine analogs.

A number of structurally significant absorption bands are present in the infrared spectrum of the DMSO adduct (middle spectrum of Figure 4). We observe that the broad band at 850 cm^{-1} has disappeared. This spectral change confirms that the $Fe_2(OH)_2$ bridging unit has been significantly altered in the reaction of DMSO with $[Fe(C_4O_4)(H_2O)_2(OH)]_2 \cdot 2H_2O$. Another striking feature of the spectrum is the appearance of a broad band at 550 cm^{-1}. We assign this absorption band to the asymmetric Fe_3O stretching mode, $\nu_{asym}(Fe_3O)$, in agreement with previous work on similar structures [19,29]. The spectrum of this material also contains a number of weak bands which we have assigned to coordinated DMSO molecules.

Positions of these bands are noted in the middle spectrum of Figure 4 by the use of a stick diagram.

The bottom tracing in Figure 4 shows the spectrum of $[Fe(C_4O_4)(H_2O)_2]_2O$. This relatively simple spectrum has certain features which are similar to those found in the other ferric squarate complexes. In particular the broad, structured band at 3300 cm^{-1} is assigned to the O-H stretch of coordinated water and the intense band envelope near 1480 cm^{-1} is assigned to C=C and C=O stretching modes of the squarate ligand. A number of weak absorptions, whose assignments are uncertain, appear below 1100 cm^{-1}. However, we observe a new, moderately intense absorption near 750 to 820 cm^{-1}. We assign these bands to the asymmetric Fe_2O stretching mode in analogy with previous workers [25,30].

Proposed Structures

On the basis of magnetic susceptibility, Mössbauer, and infrared evidence (vide supra) we propose structures for these new squarate complexes which are consistent with the data. It is clear that the products of the reaction of pyridine-like bases with $[Fe(C_4O_4)(H_2O)_2$ $(OH)]_2 \cdot 2H_2O$ have similar properties to the aquo complex. The most likely structure (6) for these complexes contains the $Fe_2(OH)_2$ bridging unit.
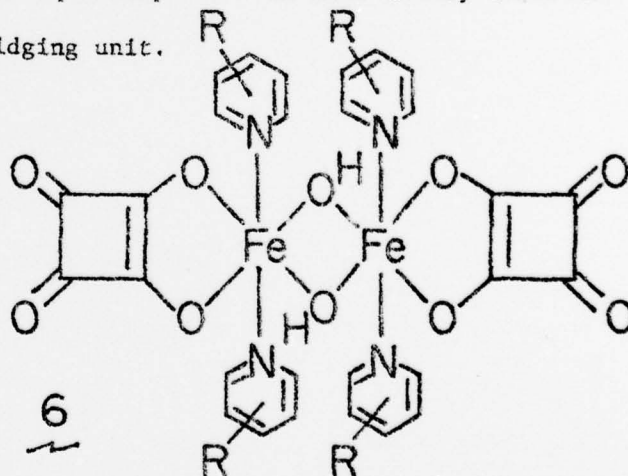
We propose a structure for the DMSO reaction product which contains the Fe_3O core (7). Although we have no information regarding precise details of the specific coordination about the iron ions, it seems likely to assume that the irons are five coordinate because of the large steric requirements of the DMSO ligands. If this structure is correct, it represents the first example of a bridging bidentate squarate ion.

7
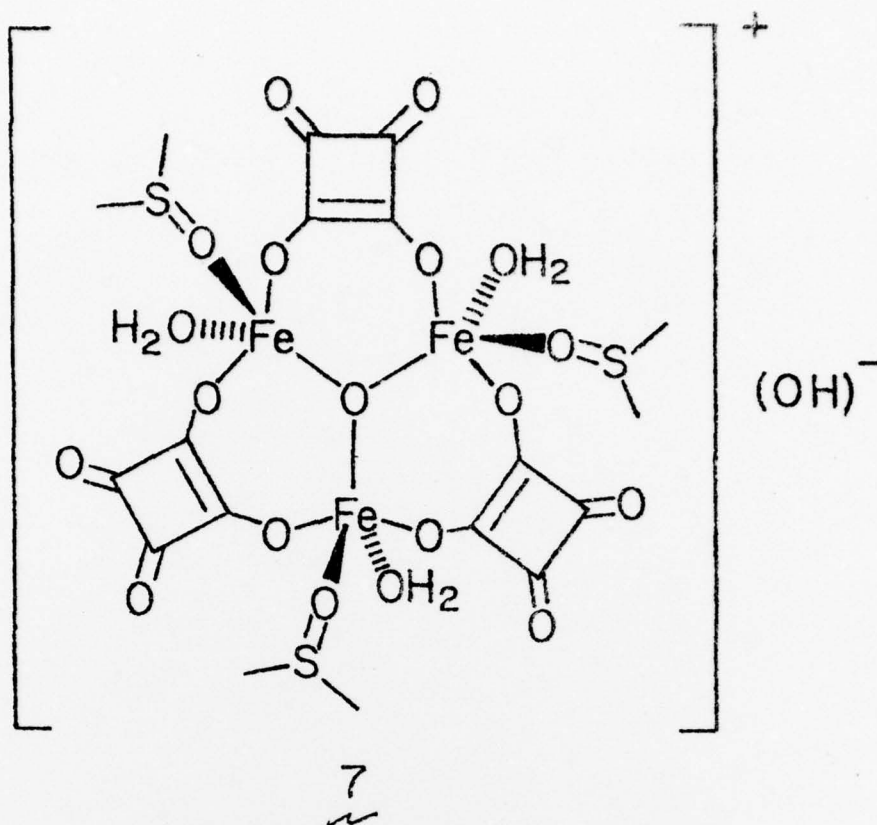
Finally, we believe the essential features of structure 8 account for the properties of the KOH reaction product. The large value of $|\underline{J}|$ by itself strongly indicates the presence of an oxo bridge, although the details of the structure are not immediately obvious from this work.
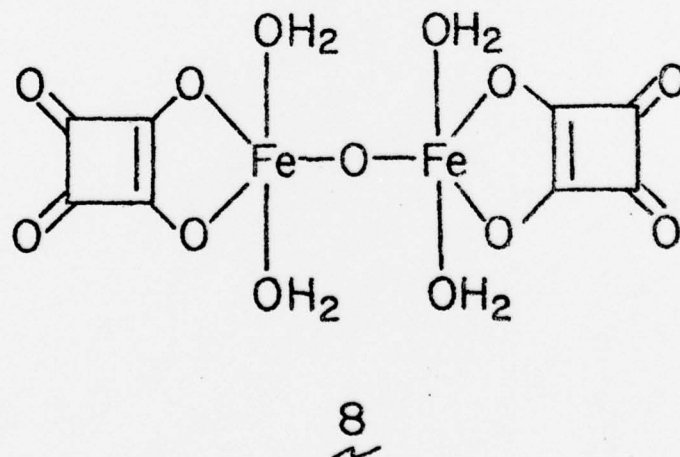
8

Acknowledgments

References

1. J. T. Wrobleski and D. B. Brown, Inorg. Chem., 17, 2959 (1978).

2. DMSO is dimethyl sulfoxide, $(CH_3)_2SO$.

3. R. West and H. Y. Niu, J. Am. Chem. Soc., 85, 2589 (1963) and H. Y. Niu, Ph.D. Dissertation, University of Wisconsin, 1962.

4. S. M. Condren and H. O. McDonald, Inorg. Chem., 12, 57 (1973).

5. J. M. Land, personal communication to JTW.

6. T. R. Felthouse, E. J. Laskowski, and D. N. Hendrickson, Inorg. Chem., 16, 1077 (1977).

7. J. T. Wrobleski and D. B. Brown, Inorg. Chem., in preparation.

8. M. Habenschuss and B. C. Gerstein, J. Chem. Phys., 61, 852 (1974).

9. G. J. Long, Inorg. Chem., 17, 2702 (1978).

10. C. W. Allen and D. B. Brown, Inorg. Chem., 13, 2020 (1974).

11. J. T. Wrobleski and D. B. Brown, Inorg. Chem., 18, 0000 (1979).

12. D. B. Brown, V. H. Crawford, J. W. Hall, and W. E. Hatfield, J. Phys. Chem., 81, 1303 (1977).

13. F. E. Mabbs and D. J. Machin, "Magnetism and Transition Metal Complexes," Chapman and Hall, London, 1973, p. 5.

14. A. P. Ginsberg, Inorg. Chim. Acta Rev., 5, 45 (1971).

15. C. C. Ou, R. A. Lalancette, J. A. Potenza, and H. J. Schugar, J. Am. Chem Soc., 100, 2053 (1978).

16. Dipic = 2,6-pyridinedicarboxylate and Chel = 4-hydroxo-2,6-pyridinedicarboxylate: J. A. Thich, C. C. Ou, D. Powers, B. Vasiliou, D. Mastropaolo, J. A. Potenza, and H. J. Schugar, J. Am. Chem. Soc., 98, 1425 (1976).

17. salgly = salicylideneglycinate: G. J. Long, J. T. Wrobleski, and G. Longworth, 176th National ACS Meeting, Abstr. of papers, #INOR 108, 1978.

18. H. J. Schugar, G. R. Rossman, and H. B. Gray, J. Am. Chem. Soc., 91, 4564 (1969).

19. See for example: G. J. Long, W. T. Robinson, W. P. Tappmeyer, and D. L. Bridges, J. Chem. Soc., Dalton Trans., 573 (1973) [$J = -28.7$ cm^{-1} for $[Fe_3O(CH_3CO_2)_6(H_2O)_3]Cl \cdot 5H_2O$] and references therein. See also C. T. Dziobkowski, J. T. Wrobleski, and

D. B. Brown, Abstracts of papers, 8th Northeast Regional ACS Meeting, paper #INOR 17, 1978 for a discussion of magnetic exchange effects in Fe(III) mono- and dicarboxylic acid trimers.

20.   Reference 13, p. 195.

21.   C. C. Ou, R. G. Wollmann, D. N. Hendrickson, J. A. Potenza, and H. J. Schugar, J. Am. Chem. Soc., 100, 4717 (1978).

22.   M. G. B. Drew, V. McKee, and S. M. Nelson, J. Chem. Soc., Dalton Trans., 80 (1978).

23.   W. M. Reiff, W. A. Baker, Jr., and N. E. Erickson, J. Am. Chem. Soc., 90, 4794 (1968).

24.   J. Lewis, F. E. Mabbs, and A. Richards, J. Chem. Soc. (A), 1014 (1967).

25.   K. S. Murray, Coord. Chem. Revs., 12, 1 (1974).

26.   N. N. Greenwood and T. C. Gibb, "Mössbauer Spectroscopy," Chapman and Hall Ltd., London, 1971.

27.   W. M. Reiff, J. Chem. Phys., 54, 4718 (1971).

28.   D. Powers, G. R. Rossman, H. J. Schugar, and H. B. Gray, J. Solid State Chem., 13, 1 (1975).

29.   The symmetric Fe_3O stretch is predicted to occur near 160 cm^{-1} while the asymmetric Fe_3O stretch has been observed and predicted near 520 cm^{-1}. See W. P. Griffith, J. Chem. Soc. (A), 2270 (1969).

30.   See, for example, A. V. Khedekar, J. Lewis, F. E. Mabbs, and H. Weigold, J. Chem. Soc., London, 1561 (1967).
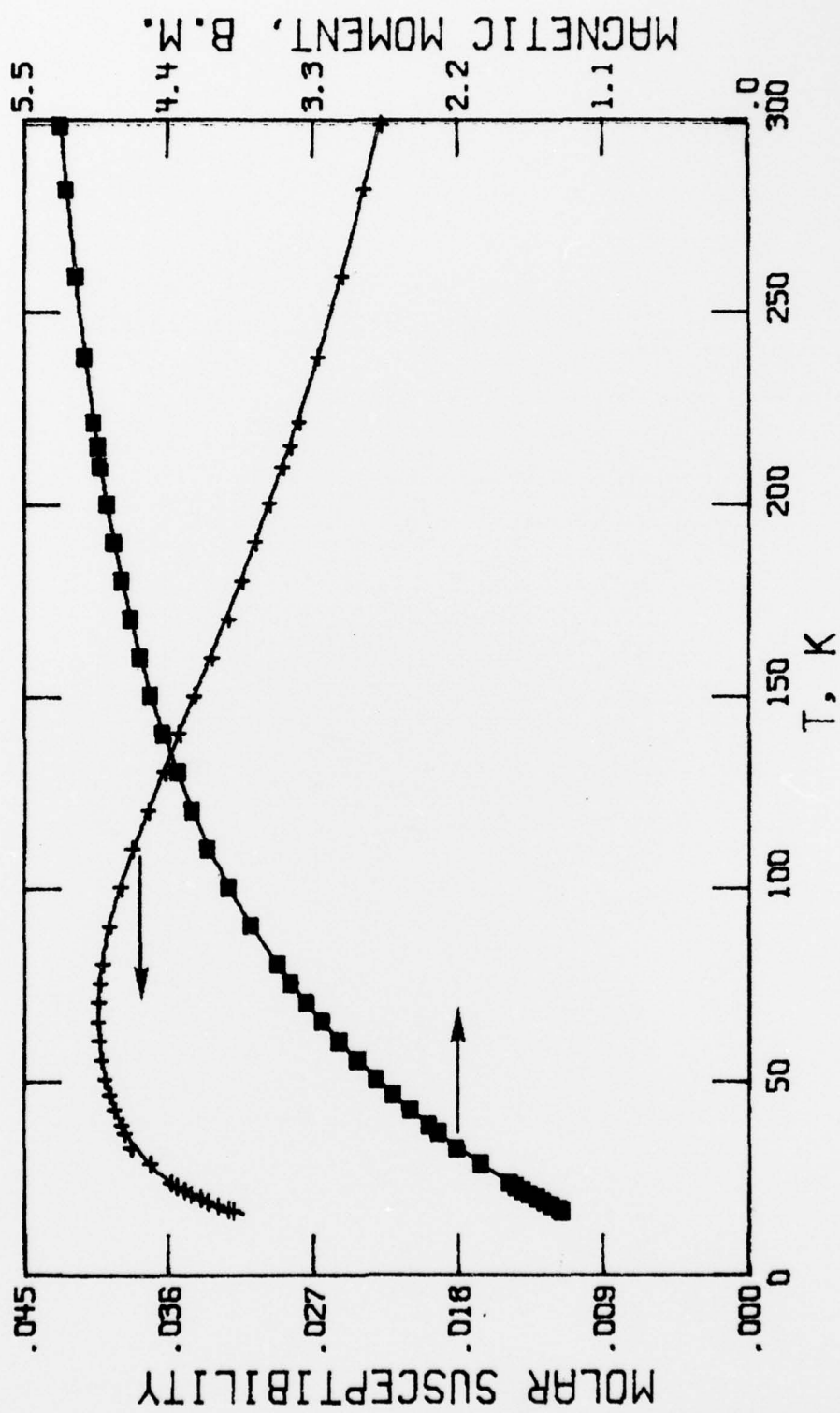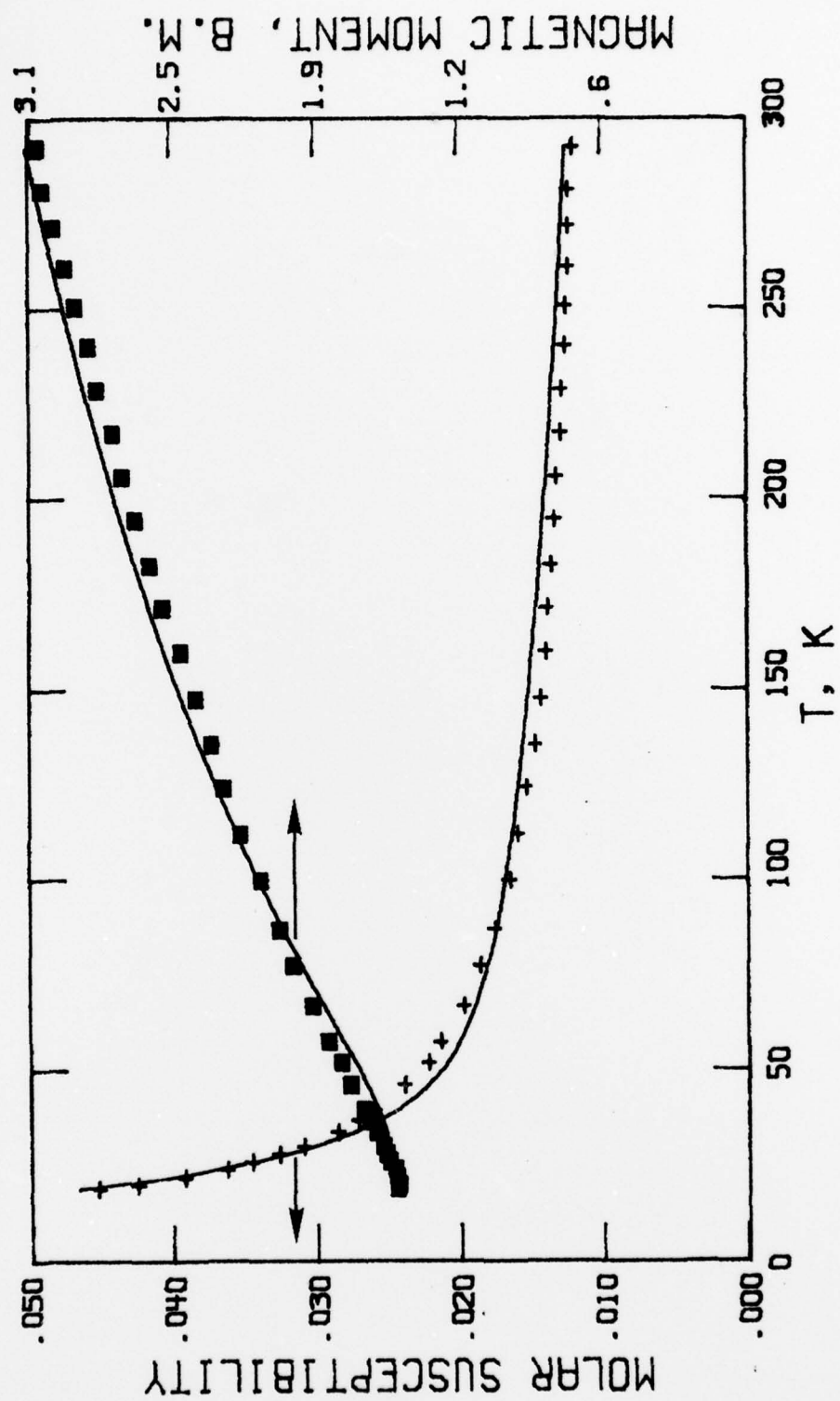
Figure Captions

Figure 1.   Experimental magnetic susceptibility (+) and effective magnetic moment per iron (●) for polycrystalline $[Fe(C_4O_4)(py)_2(OH)]_2 \cdot 2H_2O$. The smooth curves are calculated from the appropriate $\underline{S}_1 = \underline{S}_2 = 5/2$ HDVV spin-exchange model with $\underline{J} = -8.0$ cm^{-1} and $g = 2.00$.

Figure 2.   Experimental magnetic susceptibility (+) and effective magnetic moment per iron (●) for polycrystalline $[Fe_3O(C_4O_4)(DMSO)_3(H_2O)_3](OH)$. The smooth curves are calculated from the appropriate $\underline{S}_1 = \underline{S}_2 = \underline{S}_3 = 5/2$ HDVV spin-exchange model (eqn. 2) with $\underline{J} = -39.0$ cm^{-1}, $g = 2.00$, and $\underline{Z} = 0.96$.

Figure 3.   Experimental magnetic susceptibility (+) and effective magnetic moment per iron (●) for polycrystalline $[Fe(C_4O_4)(H_2O)_2]_2O$. The smooth curves are calculated from the appropriate $\underline{S}_1 = \underline{S}_2 = 5/2$ HDVV spin-exchange model with $J = -96$ cm^{-1} and $g = 2.00$

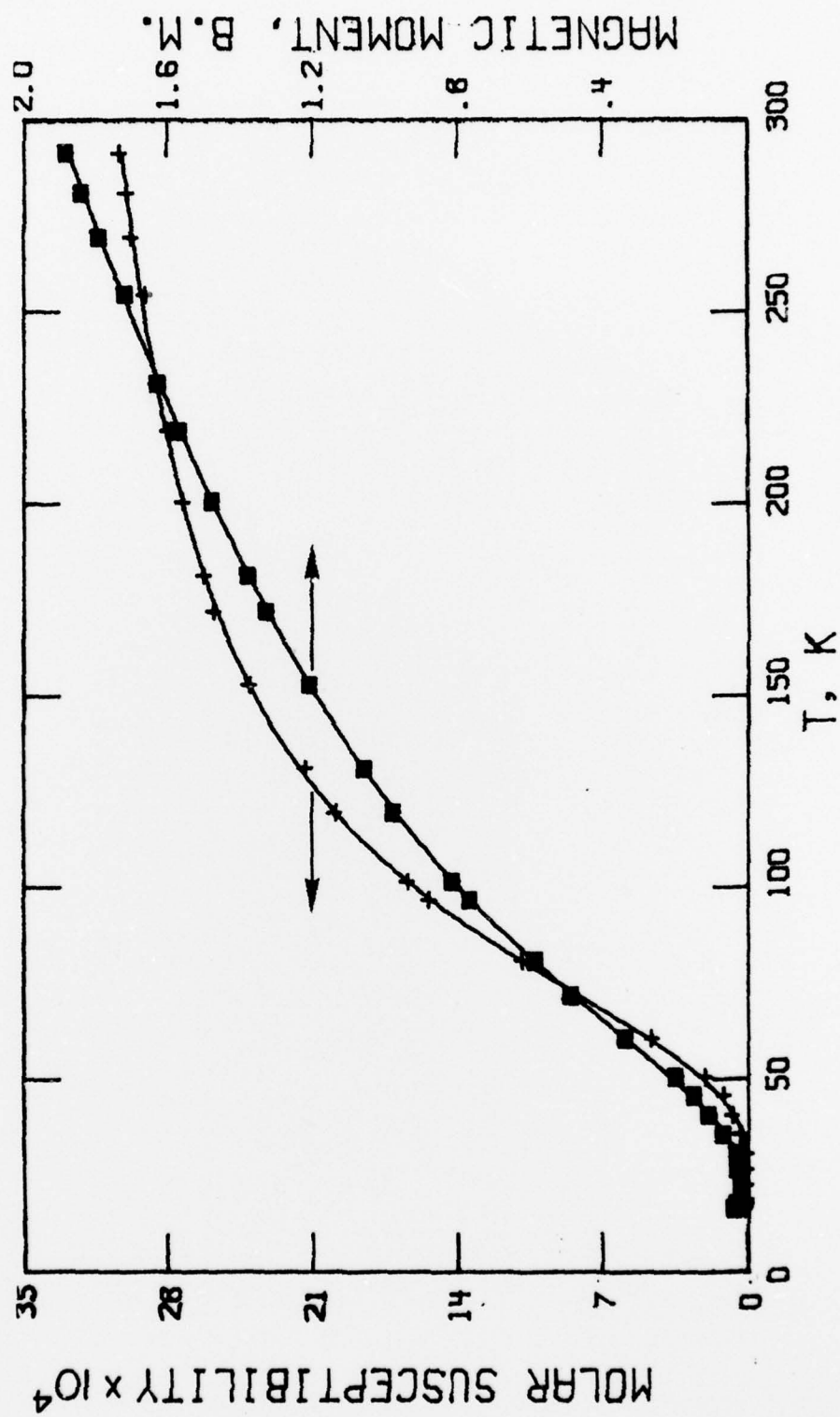Figure 4.   Infrared spectra (4000-250 cm^{-1}) taken in KBr pressed pellets.

% Transmission

$[Fe(C_4O_4)(H_2O)_2(OH)]_2 \cdot 2H_2O$

850

DMSO

$[Fe_3O(C_4O_4)_3(DMSO)_3(H_2O)_3](OH)$

550

$[Fe(C_4O_4)(H_2O)_2]_2O$

820
780

Wavenumber, cm^{-1}

400   600   800   1000   1200   1400   1600   1800   2000   2500   3000   3500   4000
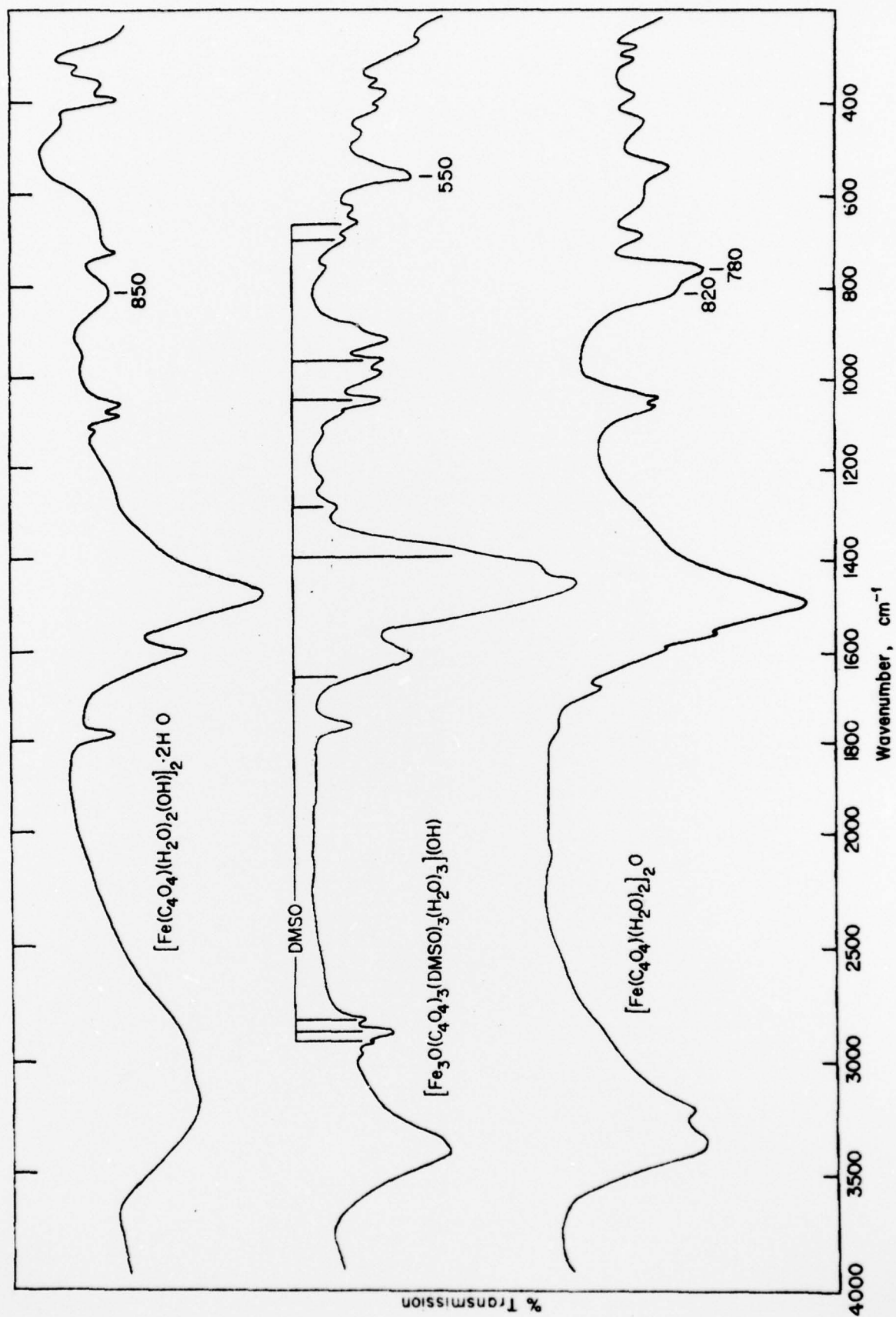
TECHNICAL REPORT DISTRIBUTION LIST, GEN

Office of Naval Research
800 North Quincy Street
Arlington, Virginia   22217
Attn: Code 472   2

ONR Branch Office
536 S. Clark Street
Chicago, Illinois 60605
Attn: Dr. George Sandoz   1

ONR Branch Office
715 Broadway
New York, New York 10003
Attn: Scientific Dept.   1

ONR Branch Office
1030 East Green Street
Pasadena, California 91106
Attn: Dr. R. J. Marcus   1

ONR Area Office
One Hallidie Plaza, Suite 601
San Francisco, California 94102
Attn: Dr. P. A. Miller   1

ONR Branch Office
Building 114, Section D
666 Summer Street
Boston, Massachusetts 02210
Attn: Dr. L. H. Peebles   1

Director, Naval Research Laboratory
Washington, D. C. 20390
Attn: Code 6100   1

The Assistant Secretary
  of the Navy (R,E&S)
Department of the Navy
Room 4E736, Pentagon
Washington, D. C.   20350   1

Commander, Naval Air Systems Command
Department of the Navy
Washington, D. C. 20360
Attn: Code 310C (H. Rosenwasser)   1

Defense Documentation Center
Building 5, Cameron Station
Alexandria, Virginia 22314   12

U. S. Army Research Office
P. O. Box 1211
Research Triangle Park, N.C. 27709
Attn: CRD-AA-IP   1

Naval Ocean Systems Center
San Diego, California 92152
Attn: Mr. Joe McCartney   1

Naval Weapons Center
China Lake, California 93555
Attn: Dr. A. B. Amster
        Chemistry Division   1

Naval Civil Engineering Laboratory
Port Hueneme, California 93401
Attn: Dr. R. W. Drisko   1

Professor K. E. Woehler
Department of Physics & Chemistry
Naval Postgraduate School
Monterey, California   93940   1

Dr. A. L. Slafkosky
Scientific Advisor
Commandant of the Marine Corps
  (Code RD-1)
Washington, D. C. 20380   1

Office of Naval Research
800 N. Quincy Street
Arlington, Virginia   22217
Attn: Dr. Richard S. Miller   1

Naval Ship Research and Development
  Center
Annapolis, Maryland 21401
Attn: Dr. G. Bosmajian
        Applied Chemistry Division   1

Naval Ocean Systems Center
San Diego, California 91232
Attn: Dr. S. Yamamoto, Marine
        Sciences Division   1

	No. Copies		No. Copies
Dr. R. N. Grimes University of Virginia Department of Chemistry Charlottsville, Virginia 22901	1	Dr. M. H. Chisholm Department of Chemistry Indiana University Bloomington, Indiana 47401	1
Dr. M. Tsutsui Texas A&M University Department of Chemistry College Station, Texas 77843	1	Dr. B. Foxman Brandeis University Department of Chemistry Waltham, Massachusetts 02154	1
Dr. M. F. Hawthorne University of California Department of Chemistry Los Angeles, California 90024	1	Dr. T. Marks Northwestern University Department of Chemistry Evanston, Illinois 60201	1
Dr. W. B. Fox Naval Research Laboratory Chemistry Division Code 6130 Washington, D. C. 20375	1	Dr. G. Geoffrey Pennsylvania State University Department of Chemistry University Park, Pennsylvania 16802	1
Dr. J. Adcock University of Tennessee Department of Chemistry Knoxville, Tennessee 37916	1	Dr. J. Zuckerman University of Oklahoma Department of Chemistry Norman, Oklahoma 73019	1
Dr. A. Cowley University of Texas Department of Chemistry Austin, Texas 78712	1	Professor O. T. Beachley Department of Chemistry State University of New York Buffalo, New York 14214	1
Dr. W. Hatfield University of North Carolina Department of Chemistry Chapel Hill, North Carolina 27514	1	Professor P. S. Skell Department of Chemistry The Pennsylvania State University University Park, Pennsylvania 16802	1
Dr. D. Seyferth Massachusetts Institute of Technology Department of Chemistry Cambridge, Massachusetts 02139	1	Professor K. M. Nicholas Department of Chemistry Boston College Chestnut Hill, Massachusetts 02167	1